Journal of Inorganic and General Chemistry

ZAAC

Zeitschrift für anorganische und allgemeine Chemie

2018

644/4

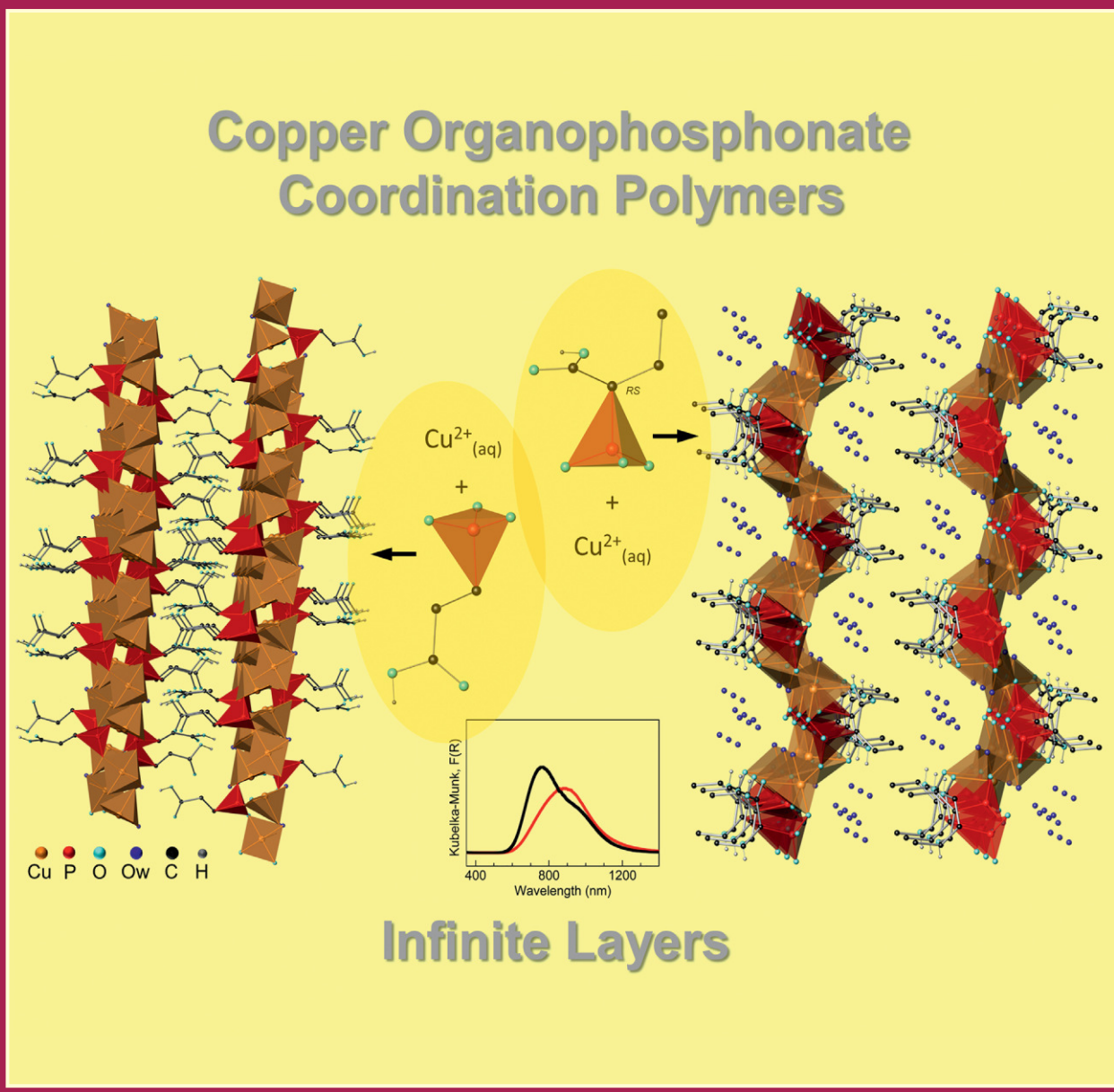

Front Cover: Crystal Structure and Characterization of Two Layered Copper(II) Coordination Polymers with Anions of 3-Phosphonopropionic Acid and (*RS*)-2-Phosphonobutyric Acid

Roberto Köferstein, Michael Arnold, and Christian Robl

WILEY-VCH

www.zaac.wiley-vch.de

Z. Anorg. Allg. Chem. 644 (2018) 205-214.

DOI: 10.1002/zaac.201700453

Crystal Structure and Characterization of Two Layered Copper(II) Coordination Polymers with Anions of 3-Phosphonopropionic Acid and (*RS*)-2-Phosphonobutyric Acid

Roberto Köferstein,[b] Michael Arnold,[a] and Christian Robl*[a]

[a] Institute of Inorganic and Analytical Chemistry, Friedrich-Schiller-University Jena, Humboldtstrasse 8, 07743 Jena, Germany
[b] Institute of Chemistry, Inorganic Chemistry, Martin Luther University Halle-Wittenberg, Kurt-Mothes-Strasse 2, 06120 Halle, Germany

Abstract: Blue single crystals of $Cu[\mu_3\text{-}O_3P(CH_2)_2COOH]\cdot 2H_2O$ (**1**) and $Cu[(RS)\text{-}\mu_3\text{-}O_3PCH(C_2H_5)COOH]\cdot 3H_2O$ (**2**) have been prepared in aqueous Cu^{2+}-solutions (pH = 2.5–3.5) containing 3-phosphonopropionic acid (**1**) and (*RS*)-2-phosphonobutyric acid (**2**), respectively. **1**: Space group Pbca (no. 61) with a = 812.5(2), b = 919.00(9), c = 2102.3(2) pm. Cu^{2+} is five-fold coordinated by three oxygen atoms stemming from $[O_3P(CH_2)_2COOH]^{2-}$ anions and two water molecules. The Cu–O bond lengths range from 194.0(3) to 231.8(4) pm. The connection between the $[O_3P(CH_2)_2COOH]^{2-}$ anions and the Cu^{2+} cations yields a polymeric structure with layers parallel to (001). The layers are linked by hydrogen bonds. **2**: Space group Pbca (no. 61) with a = 1007.17(14), b = 961.2(3), c = 2180.9(4) pm. The copper cations are surrounded by five oxygen atoms in a square pyramidal fashion with Cu–O bonds between 193.6(4) and 236.9(4) pm. The coordination between $[O_3PCH(C_2H_5)COOH]^{2-}$ and Cu^{2+} results in infinite puckered layers parallel to (001). The layers are not connected by any hydrogen bonds. Each layer contains both *R* and *S* isomers of the $[O_3PCH(C_2H_5)COOH]^{2-}$ dianion. Water molecules not bound to Cu^{2+} are intercalated between the layers. UV/Vis spectra suggest three d–d transition bands at 743, 892, 1016 nm for **1** and four bands at 741, 838, 957 and 1151 nm for **2**, respectively. Magnetic measurements suggest a weak antiferromagnetic coupling between Cu^{2+} due to a super-superexchange interaction. Thermoanalytical investigations in air show that the compounds are stable up to 95 °C (**1**) and 65 °C (**2**), respectively.

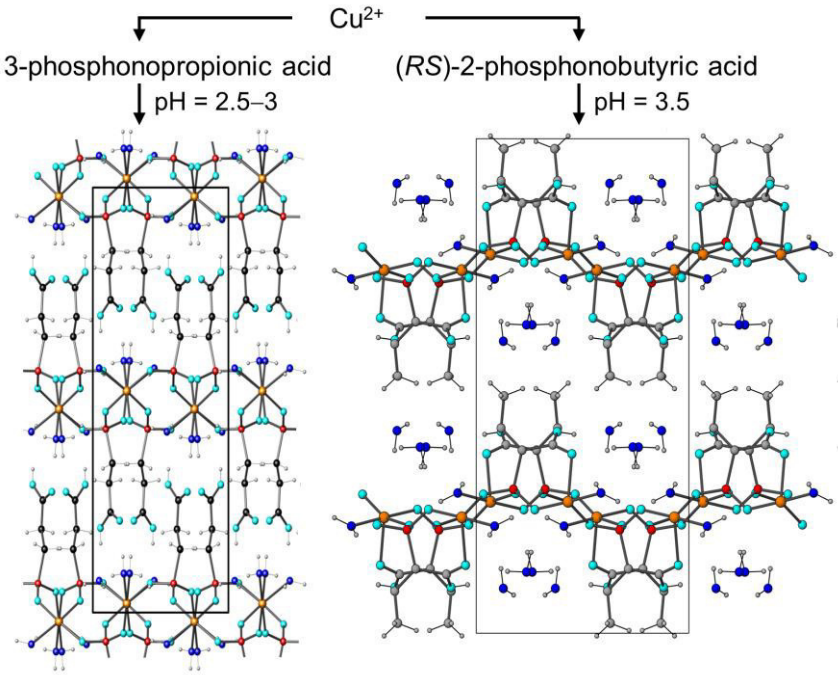

Crystal Structure and Characterization of Two Layered Copper(II) Coordination Polymers with Anions of 3-Phosphonopropionic Acid and (*RS*)-2-Phosphonobutyric Acid

Roberto Köferstein[b], Michael Arnold[a], and Christian Robl*[a]

Dedicated to Prof. Dr. Wolfgang Weigand on the occasion of his 60th birthday.

Abstract: Blue single crystals of $Cu[\mu_3\text{-}O_3P(CH_2)_2COOH]\cdot 2H_2O$ (**1**) and $Cu[(RS)\text{-}\mu_3\text{-}O_3PCH(C_2H_5)COOH]\cdot 3H_2O$ (**2**) have been prepared in aqueous Cu^{2+}-solutions (pH = 2.5–3.5) containing 3-phosphonopropionic acid (**1**) and (*RS*)-2-phosphonobutyric acid (**2**), respectively. **1**: Space group Pbca (no. 61) with *a* = 812.5(2), *b* = 919.00(9), *c* = 2102.3(2) pm. Cu^{2+} is five-fold coordinated by three oxygen atoms stemming from $[O_3P(CH_2)_2COOH]^{2-}$ anions and two water molecules. The Cu–O bond lengths range from 194.0(3) to 231.8(4) pm. The connection between the $[O_3P(CH_2)_2COOH]^{2-}$ anions and the Cu^{2+} cations yields a polymeric structure with layers parallel to (001). The layers are linked by hydrogen bonds. **2**: Space group Pbca (no. 61) with *a* = 1007.17(14), *b* = 961.2(3), *c* = 2180.9(4) pm. The copper cations are surrounded by five oxygen atoms in a square pyramidal fashion with Cu–O bonds between 193.6(4) and 236.9(4) pm. The coordination between $[O_3PCH(C_2H_5)COOH]^{2-}$ and Cu^{2+} results in infinite puckered layers parallel to (001). The layers are not connected by any hydrogen bonds. Each layer contains both *R* and *S* isomers of the $[O_3PCH(C_2H_5)COOH]^{2-}$ dianion. Water molecules not bound to Cu^{2+} are intercalated between the layers. UV/Vis spectra suggest three d–d transition bands at 743, 892, 1016 nm for **1** and four bands at 741, 838, 957 and 1151 nm for **2**, respectively. Magnetic measurements suggest a weak antiferromagnetic coupling between Cu^{2+} due to a super-superexchange interaction. Thermoanalytical investigations in air show that the compounds are stable up to 95 °C (**1**) and 65 °C (**2**), respectively.

Introduction

Metal organophosphonate complexes are of great interest due to their potential application e.g. as gas sensor[1], catalyst[2,3], and ion exchanger[4]. Zinc 5-phosphonobenzene-1,3-dicarboxylate acts as catalyst in Friedel-Crafts benzylation reactions and a selective CO_2 uptake was observed for cobalt uranyl phosphonoacetate and indium 4'-phosphonobiphenyl-3,5-dicarboxlyate.[5–8] Ion exchange properties were found for e.g. titanium-, chromium-, and aluminum 3-phosphonohydrogenpropionate and zirconium diphosphonate-phosphate hybrids, whereas cobalt 1-(methylenephosphono)-pyrrolidine-2-carboxylate can be used as catalyst for water oxidation.[9-12] The coordination between bifunctional phosphonocarboxylates and metal cations leads to various structural motives.[13–18] In complex compounds the anion of e.g. phosphonopropionic acid appears in its monoanionic, dianionic, and trianionic form depending on synthesis conditions. Three-dimensional open frameworks are reported for the connection between 3-phosphonopropionate anions and e.g. divalent Co, Cu, Zn, Pb, and Sn cations.[13,18–22] Coordination to Ti^{4+}, Al^{3+}, Cr^{3+}, Cd^{2+}, $Mn^{2+/3+}$ and Fe^{2+} leads to layer-like structures.[9,10,17,23,24] Using additional N-donor ligands, chain-like coordination polymers are available.[25–27]

To our best knowledge, up to date crystal structures of metal complexes containing the anions of 2-phosphonobutyric acid have not been reported yet.

Herein, we report on the crystal structures and properties of two layer-like copper(II) coordination polymers with the dianion of 3-phosphonopropionic acid ($Cu[\mu_3\text{-}O_3P(CH_2)_2COOH]\cdot 2H_2O$) and 2-phosphonobutyric acid ($Cu[(RS)\text{-}\mu_3\text{-}O_3PCH(C_2H_5)COOH]\cdot 3H_2O$), respectively. Due to their COOH groups, these compounds may act as cation exchangers.

Results and Discussion

$Cu[\mu_3\text{-}O_3P(CH_2)_2COOH]\cdot 2H_2O$ (1)

In $Cu[\mu_3\text{-}O_3P(CH_2)_2COOH]\cdot 2H_2O$ (**1**) the Cu^{2+} cations occupy the general position of space group Pbca. The copper cations are coordinated by five oxygen atoms in a slightly distorted square pyramidal fashion (Figure 1). Three phosphonate oxygen atoms [O(3), O(4) O(5)], from three crystallographically equivalent $[O_3P(CH_2)_2COOH]^{2-}$ dianions and the water molecule O(w2) form the equatorial plane. The Cu–O distances range from 194.0(3) to 200.2(3) pm (Table 1). The best least-square-plane through Cu, O(3), O(4), O(5), and O(w2) reveals only a slight deviation from planarity with an average and maximum deviation of 4.2 and 8.6 pm, respectively. The apical position is occupied by the water molecule O(w1) with a bond length of 231.8(4) pm. The bond angles within the polyhedron differ marginally from the

* Prof. Dr. C. Robl
Fax: +49-3641-948152
E-mail: crr@uni-jena.de
[a] Institute of Inorganic and Analytical Chemistry
Friedrich-Schiller-University Jena
Humboldtstrasse 8, 07743 Jena, Germany
[b] Institute of Chemistry, Inorganic Chemistry
Martin Luther University Halle-Wittenberg
Kurt-Mothes-Strasse 2
06120 Halle, Germany

Supporting information for this article is available on the WWW under **http://dx.doi.org/10.1002/zaac.201000xxx** or from the author.

ideal values. According to *Hathaway*[28,29] and *Pasquarello* et al.[30] Cu–O distances up to 300 pm (sum of van der Waals radii) should be considered to be bonds. Considering such distances, a further phosphonate oxygen atom O(5')$^{\#2}$ in the apical position with a fairly large Cu–O distance of 295.5(3) pm can be identified (see Figure 1, thin dashed line). However, the resulting polyhedron (cn: 4+1+1) in this case would be a very strongly distorted octahedron. The angle between the apical positions [O(w1)–Cu–O(5')$^{\#2}$] is only 144.9(1)° and the angles between O(5')$^{\#2}$ and the equatorial positions range from 56.6(1)° to 117.8(1)°. Because of the large distance and the enormous deviations from the ideal octahedral angles, the interaction between the d_z^2 orbital from Cu^{2+} and orbitals from the oxygen ligand O(5')$^{\#2}$ can be neglected. Therefore, the coordination environment of Cu^{2+} is here more reasonably described as a square pyramid with an approximately C_{2v} point group symmetry. Employing the method of *Brese* and *O'Keeffe*[31] the bond order with cn 5 is calculated to 2.04.

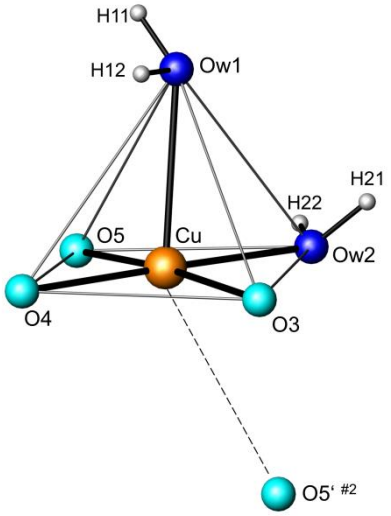

Figure 1. The square pyramidal coordination (thick black bonds) of Cu^{2+} in $Cu[\mu_3\text{-}O_3P(CH_2)_2COOH]\cdot 2H_2O$ (**1**). The index (') indicates the longest Cu–O distance. Symmetry code #2: x-0.5; -y+1.5; -z+1.

Table 1. The coordination of Cu^{2+} in $Cu[\mu_3\text{-}O_3P(CH_2)_2COOH]\cdot 2H_2O$ (**1**)

Distances (pm)			
Cu–O(3)	194.7(3)	Cu–O(w2)	200.2(3)
Cu–O(4)	196.1(3)	Cu–O(w1)	231.8(4)
Cu–O(5)	194.0(3)		
		Cu···Cu$^{\#4}$	459.5(1)
Bond angles (°)			
O(3)–Cu–O(4)	90.8(2)	O(4)–Cu–O(w2)	178.9(2)
O(5)–Cu–O(4)	91.08(14)	O(4)–Cu–O(w1)	95.8(2)
O(3)–Cu–O(w2)	89.4(2)	O(5)–Cu–O(w1)	93.4(2)
O(5)–Cu–O(w2)	88.64(14)	O(3)–Cu–O(w1)	91.72(13)
O(5)–Cu–O(3)	174.31(14)	O(w2)–Cu–O(w1)	85.3(2)

Symmetry code: #4: 0.5-x; -0.5+y; z

The phosphonate group in the dianion of the 3-phosphonopropionic acid $[O_3P(CH_2)_2COOH]^{2-}$ is completely deprotonated. The phosphorus atom is surrounded in a distorted tetrahedral fashion by three oxygen atoms and one carbon atom (Figure 2a). The P–O bond lengths are between 151.9(3) and 153.4(3) pm, whereas the P–C bond is 180.3(5) pm (Table 2). The bonds within the COOH group show typical values for single and double bonded oxygen atoms.[32] The C–O bond length to the carbonyl oxygen atom is 121.0(7) pm [C(3)–O(2)] and to the hydroxyl oxygen atom is 131.3(7) pm [C(3)–O(1)]. The carboxyl group is twisted against the carbon skeleton C(1)–C(2)–C(3) by 21.8(5)°. As seen in Figure 2b the $[O_3P(CH_2)_2COOH]^{2-}$ dianion shows an antiperiplanar (–ap) conformation. Each dianion coordinates only with the phosphonate group to the three Cu^{2+} cations in a monodentate manner and adopts a $\mu_3\text{-}\eta_1{:}\eta_1{:}\eta_1$ coordination mode. The carboxyl group is not involved in any Cu–O bonds in contrast to other copper 3-phosphonopropionate coordination polymers.[20,25,33,34]

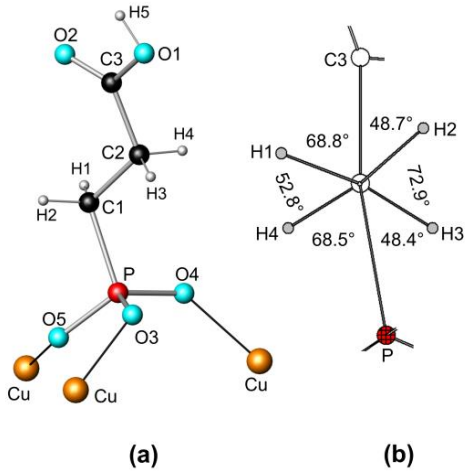

Figure 2. (a) The connection between the dianion of the 3-phosphonopropionic acid and the Cu^{2+} cations in $Cu[\mu_3\text{-}O_3P(CH_2)_2COOH]\cdot 2H_2O$ (**1**). (b) Newman projection of the $[O_3P(CH_2)_2COOH]^{2-}$ dianion along C(1)–C(2).

Table 2. Bond lengths and angles of the $[O_3P(CH_2)_2COOH]^{2-}$ anion in $Cu[\mu_3\text{-}O_3P(CH_2)_2COOH]\cdot 2H_2O$ (**1**)

Distances (pm)			
P–O(3)	153.4(3)	C(3)–O(1)	131.3(7)
P–O(4)	151.9(3)	C(3)–O(2)	121.0(7)
P–O(5)	152.5(3)	C(1)–C(2)	152.5(7)
P–C(1)	180.3(5)	C(2)–C(3)	149.4(7)
		O(1)–H(5)	86(8)
Bond angles (°)			
O(4)–P–O(5)	114.0(2)	O(3)–P–C(1)	107.1(2)
O(5)–P–O(3)	108.8(2)	O(2)–C(3)–C(2)	125.3(6)
O(4)–P–O(3)	112.3(2)	O(1)–C(3)–C(2)	111.1(5)
O(5)–P–C(1)	108.3(2)	O(2)–C(3)–O(1)	123.6(5)
O(4)–P–C(1)	106.1(2)	C(2)–C(1)–P	112.7(4)
O(3)–P–C(1)	107.1(2)	C(3)–C(2)–C(1)	114.5(5)
		C(3)–O(1)–H(5)	102(5)

C–H: 97 pm

The copper centered polyhedra and the $[O_3PC]$ tetrahedra are alternately connected by common corners through O(3), O(4) and O(5) yielding four- and eight-membered polyhedra rings (dashed lines in Figure 3) to form infinite centrosymmetric layers, which are stacked in …ABAB… sequence along the [001] direction (Figure 4). There is no direct connection between neighbouring Cu^{2+} square pyramids. The shortest distance between adjacent polyhedra layers is 426 pm (without van-der-Waals radii taken into account). As seen in Figure 5 the propionic acid groups extend into the interlayer space along the c-axis direction.

Due to the COOH group, $Cu[\mu_3\text{-}O_3P(CH_2)_2COOH]\cdot 2H_2O$ (**1**) can be regarded as the protonated form of a cation exchanger with a layer-like structure. The theoretical exchange capacity is 4.0 mval g^{-1} and the calculated surface charge density of the deprotonated layers is $0.054\cdot 10^{-4}$ e·pm^{-2} ($18.7\cdot 10^4$ pm^2 per unit charge), which is close to the values found in layered silicates like Muscovite and Zinnwaldite.[35]

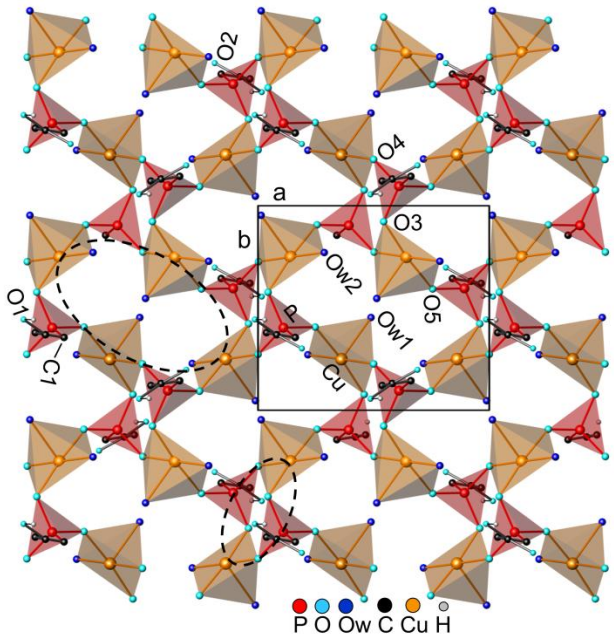

Figure 3. View on a selected layer in the (001) plane formed through the connection between the Cu^{2+} centered polyhedra and the $[O_3PC]$ tetrahedra in **1**. Hydrogen atoms from water molecules and CH_2 groups are omitted for clarity. The black dashed lines illustrate the four- and eight-membered rings formed by the copper and phosphorus centered polyhedra.

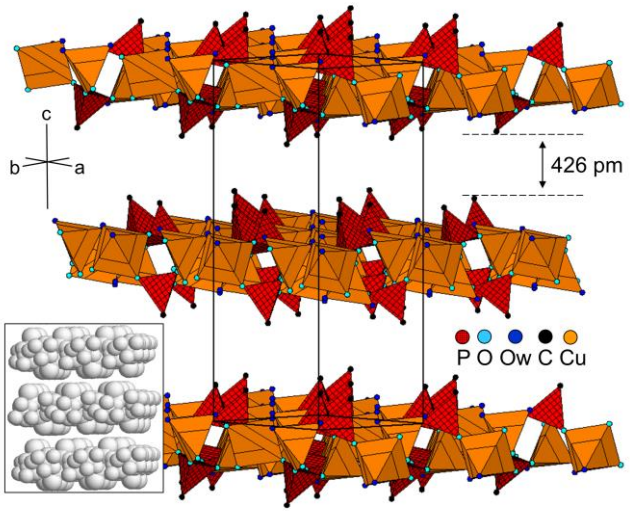

Figure 4. Stacking of the polyhedra layers along [001] in **1**. The inset shows the space-filling model.

The layers are only linked by strong and medium strength hydrogen bonds (Table 3). Here, the hydroxo group O(1)–H(5) from the carboxyl group acts as proton donator to the water molecule O(w1), whereas the carboxyl oxygen atom O(2) is the acceptor atom to O(w2) of the neighbouring layer (Figure 5).

Within the same layer the water molecules O(w1) and O(w2) are involved in weak to strong hydrogen bonds to the phosphonate oxygen atoms O(3), O(4), and O(5). A weak hydrogen bond is formed between the two water molecules.

Similar, but not identical, layered structures have been reported for *M*(OH) $[O_3P(CH_2)_2COOH]\cdot H_2O$ (*M* = Fe^{3+}, Ga^{3+}, Mn^{3+}) and $Mn[O_3P(CH_2)_2COOH]\cdot H_2O$ in which the metal coordination polyhedra are directly connected by common corners and in the latter compound the phosphonate groups act as chelate ligands.[24,36,37]

Britel et al.[20] reported on a three-dimensional copper 3-phosphonopropionate in which each anion is coordinated to six Cu^{2+} via both the phosphonate and the carboxylate group.

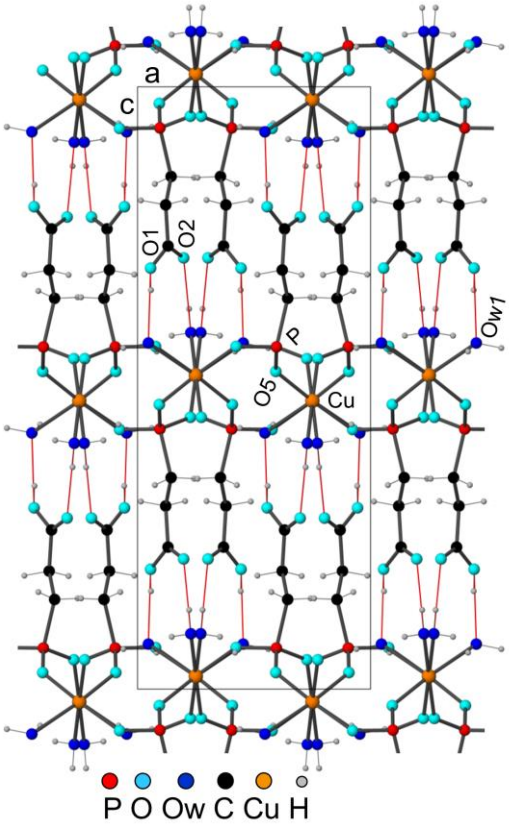

Figure 5. Complete crystal structure of **1** viewed from [010]. The interlayer hydrogen bonds are drawn by thin red lines.

Table 3. Hydrogen bonds in **1**

	O···O Distance (pm)	O-H···O Angle (°)
O(1)–H(5)···O(w1)[a]	262.6(6)	148(8)
O(w2)–H(21)···O(2)[a]	277.2(6)	178(3)
O(w2)–H(22)···O(3)	270.5(5)	149(4)
O(w1)–H(11)···O(4)	266.0(5)	177(2)
O(w1)–H(12)···O(5)	287.6(5)	123(3)
O(w1)–H(12)···O(w2)	279.5(5)	133(3)

[a] hydrogen bonds to neighbouring layers
O(w1)–H(11): 89(2) pm, O(w1)–H(12): 87(2) pm
O(w2)–H(21): 89(5) pm, O(w2)–H(22): 89(5) pm

Cu[(RS)-μ₃-O₃PCH(C₂H₅)COOH]·3H₂O (2)

The copper cations occupy the general position of space group Pbca and they are coordinated by five oxygen atoms (Figure 6). The equatorial plane is spanned by three phosphonate oxygen atoms [O(3), O(4), O(5)] from three, but crystallographically equivalent, $[\mu_3\text{-}O_3PCH(C_2H_5)COOH]^{2-}$ dianions and one water molecule [O(w1)]. The Cu–O distances are between 193.6(4) and 195.3(3) pm (Table 4). The best least-square-plane through Cu, O(3), O(4), O(5), and O(w1) shows a considerable deviation from planarity (average of 21.3 pm) with a maximum deviation of 32 pm for O(4) and O(5). The carboxyl oxygen atom O(2) occupies the axial position with a bond length of 236.9(4) pm. The bond angles within the distorted square pyramidal coordination polyhedron differ significantly from the ideal values. The copper coordination polyhedron is more distorted than in compound **1** and therefore possesses a point group symmetry lower than C_{2v}. According to *Brese* and *O'Keeffe* [31] the bond order for Cu^{2+} was calculated to 2.10.

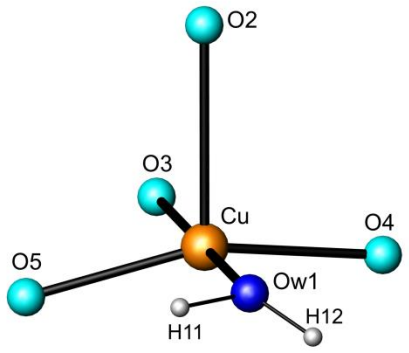

Figure 6. The coordination sphere of Cu^{2+} in $Cu[(RS)\text{-}\mu_3\text{-}O_3PCH(C_2H_5)COOH]\cdot 3H_2O$ (**2**).

Table 4. The coordination of Cu^{2+} in $Cu[(RS)\text{-}\mu_3\text{-}O_3PCH(C_2H_5)COOH]\cdot 3H_2O$ (**2**)

Distances (pm)			
Cu–O(w1)	193.6(4)	Cu–O(5)	194.6(3)
Cu–O(3)	195.0(3)	Cu–O(2)	236.9(4)
Cu–O(4)	195.3(3)		
		Cu···Cu$^{\#4}$	504.2(2)
Bond angles (°)			
O(w1)–Cu–O(5)	91.3(2)	O(w1)–Cu–O(3)	178.6(2)
O(5)–Cu–O(3)	88.13(13)	O(5)–Cu–O(2)	102.8(2)
O(w1)–Cu–O(4)	93.6(2)	O(4)–Cu–O(2)	97.0(2)
O(3)–Cu–O(4)	87.36(14)	O(w1)–Cu–O(2)	90.7(2)
O(5)–Cu–O(4)	159.6(2)	O(3)–Cu–O(2)	88.2(2)

Symmetry code: #4: -x+2; y+0.5+y; -z+0.5

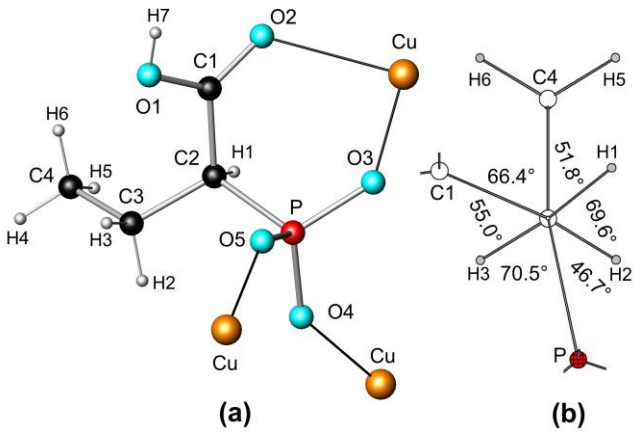

Figure 7. (a) The connection between the $[O_3PCH(C_2H_5)COOH]^{2-}$ dianion and the copper cations in **2**. (b) Newman projection of the $[O_3PCH(C_2H_5)COOH]^{2-}$ dianion along C(2)–C(3). The figures show the *S* enantiomer.

As seen in Figure 7a, each dianion of the 2-phosphonobutyric acid $[O_3PCH(C_2H_5)COOH]^{2-}$ bridges three copper cations. In contrast to compound **1**, both the $[PO_3]$ and [COOH] groups are involved in the coordination to Cu^{2+} and they adopt a $\mu_3\text{-}\eta_1\text{:}\eta_1\text{:}\eta_1$ and a $\mu_1\text{-}\eta_1$ coordination mode, respectively. The hydroxyl oxygen atom O(1) from the carboxyl group is not bonded to Cu^{2+}. The coordination of O(3) and O(2) to the same Cu^{2+} connects the phosphonate group with the carboxyl group and leads to the formation of a chelating six-membered ring [O(2)–C(1)–C(2)–P–O(3)–Cu] as found also in other copper phosphonocarboxylates.[15, 38] The P–O bond lengths in the $[CPO_3]$ tetrahedron are between 151.6(3) and 153.1(4) pm and the P–C bond is 180.8(6) pm (Table 5). The C–O bond lengths within the carboxyl group are 122.1(7) pm and 130.2(8) pm, indicating double and single bond character, respectively.[32] According to the *Klyne-Prelog* convention the *Newman* projection (Figure 7b) shows an antiperiplanar (–ap) conformation.[39] The $[O_3PCH(C_2H_5)COOH]^{2-}$ dianions appear equally in *R* and *S* configuration (see Figure 8) correlated by a centre of symmetry within one layer excluding optical activity.

Table 5. Bond length and angles of the $[O_3PCH(C_2H_5)COOH]^{2-}$ anion in $Cu[(RS)\text{-}\mu_3\text{-}O_3PCH(C_2H_5)COOH]\cdot 3H_2O$(**2**)

Distances (pm)			
P–O(3)	152.7(4)	C(1)–O(2)	122.1(7)
P–O(4)	151.6(3)	C(1)–C(2)	151.4(8)
P–O(5)	153.1(4)	C(2)–C(3)	153.6(8)
P–C(2)	180.8(6)	C(3)–C(4)	151.0(10)
C(1)–O(1)	130.2(8)	O(1)–H(7)	86(7)
Bond angles (°)			
O(4)–P–O(3)	112.9(2)	O(1)–C(1)–C(2)	115.0(6)
O(3)–P–O(5)	109.8(2)	O(2)–C(1)–C(2)	122.1(5)
O(4)–P–O(5)	111.2(2)	C(1)–C(2)–C(3)	115.4(5)
O(4)–P–C(2)	106.9(2)	C(1)–C(2)–C(3)	115.4(5)
O(3)–P–C(2)	108.5(2)	C(4)–C(3)–C(2)	113.3(6)
O(5)–P–C(2)	107.2(3)	C(1)–C(2)–P	109.0(4)
O(2)–C(1)–O(1)	122.6(6)	C(3)–C(2)–P	112.2(4)

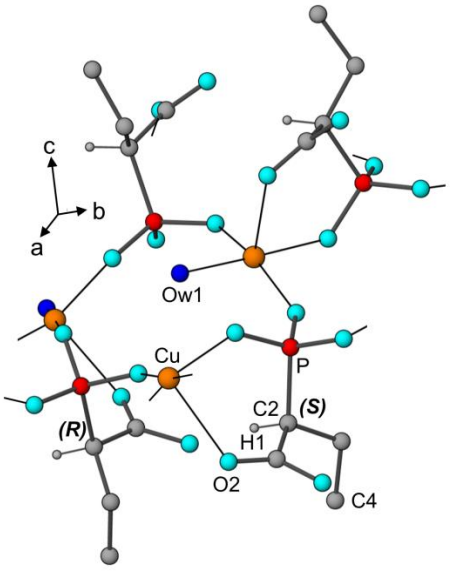

Figure 8. *R* and *S* enantiomers of the $[O_3PCH(C_2H_5)COOH]^{2-}$ dianions in the crystal structure of **2**. Hydrogen atoms [except H(1)] and the water molecules O(w2) and O(w3) are omitted for clarity.

In **2**, the coordination of the $[O_3PCH(C_2H_5)COOH]^{2-}$ dianions to the copper cations leads to puckered infinite layers extending in the (001) plane (Figure 9 and S1, Supporting Information) and they are stacked in …ABAB… sequence along the [001] direction. The layers are build up by the connection between the copper cations and the phosphonate oxygen atoms. The coordination of the carboxyl oxygen atom O(2) to Cu^{2+} only leads to a stabilization of the structure. The polyhedra around the copper atoms and the phosphorus atoms are alternately connected by common corners leading to six-membered rings (Figure 10, dashed line). Each layer contains both the *R* and *S* enantiomers of the $[O_3PCH(C_2H_5)COOH]^{2-}$ dianion in alternating sequence. In contrast to **1**, the layers are confined by the methyl group C(4) pointing towards the interlayer space along [001]. The water molecules O(w2) and O(w3), not bound to Cu^{2+}, are intercalated between the layers. Adjacent layers do not form neither O-H···O nor C-H···O interlayer hydrogen bonds between each other. The coordinated water molecule O(w1) forms weak and strong intralayer hydrogen bonds to the phosphonate oxygen atoms O(5) and O(4) (Table 6). The protonated carboxyl oxygen atom O(1) acts as proton donator in a weak hydrogen bond to O(w3). The uncoordinated water molecule O(w2) forms strong hydrogen bonds to the oxygen atoms O(2) and O(3). Between O(w2) and O(w3) there is only a weak interaction.

Analogous to **1** Cu[(*RS*)-μ_3-$O_3PCH(C_2H_5)COOH]\cdot 3H_2O$ can be regarded as the protonated form of a layered cation exchanger with a theoretical exchange capacity of 3.5 mval g^{-1} and a surface charge density of $0.041\cdot 10^{-4}$ e·pm^{-2}.

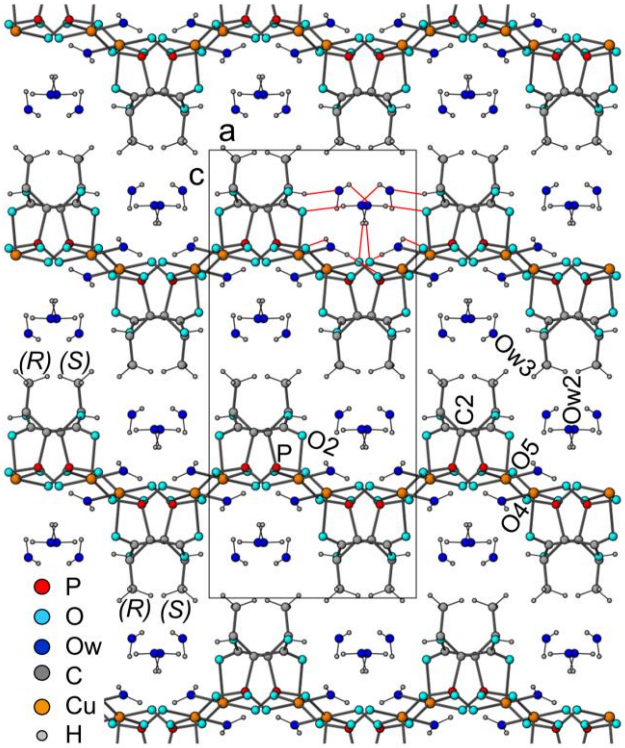

Figure 9. Crystal structure of Cu[(*RS*)-μ_3-$O_3PCH(C_2H_5)COOH]\cdot 3H_2O$ (**2**) viewed from [010]. *R* and *S* indicate the absolute configuration at the stereogenic C(2) atom. The red thin lines show a section of the hydrogen bonds. Hydrogen atoms bound to C3 [H(2), H(3)] are omitted for clarity.

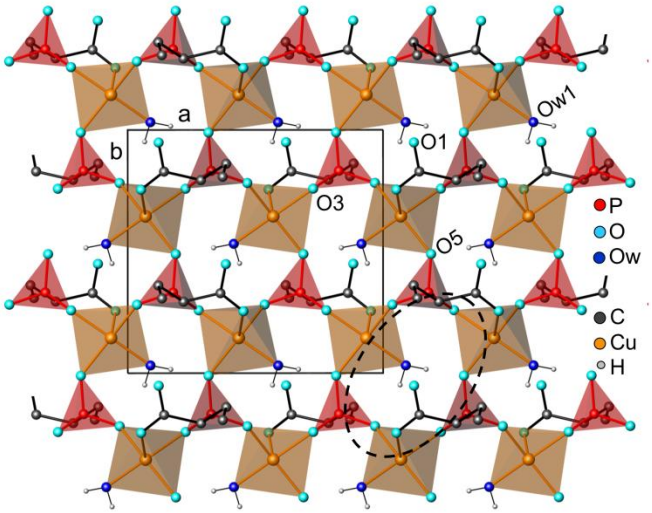

Figure 10. View on a selected layer in the (001) plane in **2**. The uncoordinated water molecules O(w2) and O(w3) and all hydrogen atoms from the $[O_3PCH(C_2H_5)COOH]^{2-}$ dianion are omitted for clarity.

Table 6. Hydrogen bonds in **2**

	O···O Distance (pm)	O-H···O Angle (°)
O(1)–H(7)···O(w3)	256.2(9)	163(7)
O(w1)–H(11)···O(4)	269.3(5)	139(3)
O(w1)–H(12)···O(5)	273.8(5)	169(1)
O(w2)–H(21)···O(3)	278.3(6)	171(2)
O(w2)–H(22)···O(2)	289.9(7)	168(2)
O(w3)–H(32)···O(w2)	281.7(9)	133(5)

O(w1)–H(11): 89(1) pm, O(w1)–H(12): 89(1) pm
O(w2)–H(21): 90(1) pm, O(w2)–H(22): 90(1) pm
O(w3)–H(31): 90(1) pm, O(w3)–H(32): 90(1) pm

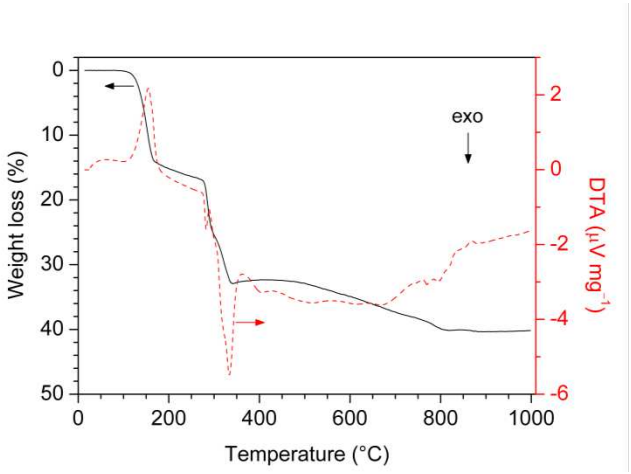

Figure 11. Thermal analysis of Cu[μ_3-$O_3P(CH_2)_2COOH$]·$2H_2O$ (**1**).

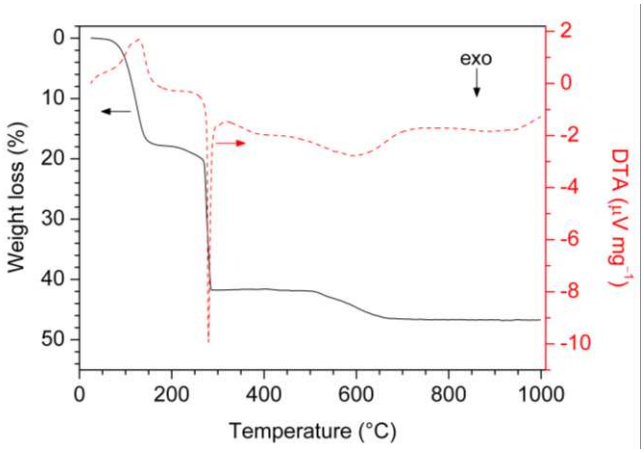

Figure 12. Thermal analysis of Cu[(*RS*)-μ_3-$O_3PCH(C_2H_5)COOH$]·$3H_2O$ (**2**).

TGA/DTA studies of Cu[μ_3-$O_3P(CH_2)_2COOH$]·$2H_2O$ (**1**) and Cu[(*RS*)-μ_3-$O_3PCH(C_2H_5)COOH$]·$3H_2O$ (**2**) were carried out in air from room temperature to 1000 °C at a heating rate of 10 K min^{-1}. With **1**, an endothermic weight loss between 95 and 175 °C of 14.3 % corresponds to the loss of all water of crystallization (calcd. 14.3 %) (Figure 11). An XRD pattern of **1** after heating to 175 °C (Figure S2, Supporting Information) shows that the loss of water is accompanied by a change of the crystal structure, because all water molecules were coordinated to Cu^{2+}. The dehydrated compound is not stable. A continuous, slight weight loss up to 270 °C leads to a total loss of 16.8 %. Two exothermic processes with onset temperatures of 276 and 289 °C cause a strong and fast decomposition step with a weight loss of 32.9 % up to 340 °C. Several following weak exothermic reactions lead to the complete decomposition up to 815 °C. The X-ray powder diffraction pattern of the residue showed reflections of $Cu_2P_2O_7$. The total weight loss of 40.3 % matches very well with the calculated one of 40.2 %.

As seen in Figure 12 the decomposition of **2** starts at 65 °C. The endothermic reaction leads to a weight loss of 18.1 % up to 212 °C, which corresponds to the loss of three water molecules per formula unit (calcd. 19.0 %). Consequently, the coordinated and uncoordinated water molecules are released simultaneously causing the crystal structure to collapse as indicated by a significant change of the XRD pattern (Figure S3, Supporting Information). Up to 272 °C a slight weight loss can be seen. A very strong exothermic decomposition reaction with an onset temperature of 274 °C causes an abrupt weight loss up to 282 °C resulting in a total loss of 41.6 %. A last decomposition step occurs between 506 and 670 °C. The white residue was identified as $Cu_2P_2O_7$ by X-ray powder diffraction. The total weight loss of 46.7 % is very close to the calculated one of 46.9 %.

Figure 13 shows the IR spectra (ATR technique) of Cu[μ_2-$OOC(CH_2)PO_3H$]·$2H_2O$ (**1**) and Cu[(*RS*)-μ_3-$O_3PCH(C_2H_5)COOH$]·$3H_2O$ (**2**). For **1**, the band at 3429 cm^{-1} and a broad band between 3400 and 2900 cm^{-1} indicate O–H stretching vibrations, whereas in **2** a broad band between 3600-3000 cm^{-1} appears. C–H stretching modes occur at 2930 cm^{-1} in **1** and at 2964, 2940, and 2881 cm^{-1} in **2**. A strong band at 1686 cm^{-1} (**1**) and 1632 cm^{-1} (**2**) is due to the C=O stretching vibration of the uncoordinated carboxylic acid group, which covers the H–O–H bending vibrations of the water molecules. Bands at 1416 cm^{-1} (**1**), 1459 and 1384 cm^{-1} (**2**) represent C–H bending vibrations. The bands at 1246, 1192, 1146, 1094, 1051 (**1**) and 1250, 1186, 1126, 1061 cm^{-1} (**2**) mainly represent P–O stretching modes.[40–42] The absorption bands at 791 and 756 cm^{-1} in **1** and 835 and 780 cm^{-1} in **2** are caused by the stretching of the P–C bond.[43,44]

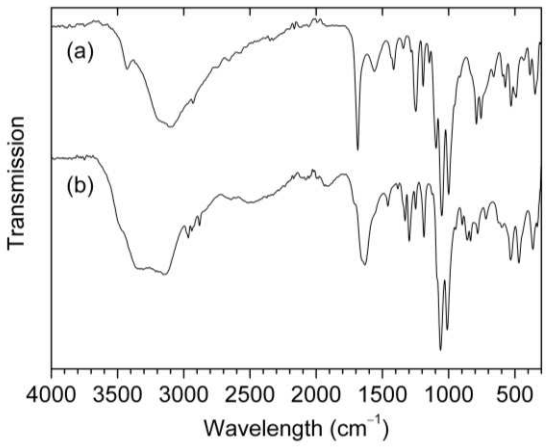

Figure 13. IR spectra of (a) Cu[μ_3-$O_3P(CH_2)_2COOH$]·$2H_2O$ (**1**) and (b) Cu[(*RS*)-μ_3-$O_3PCH(C_2H_5)COOH$]·$3H_2O$ (**2**).

Magnetic measurements were carried out between 3 and 295 K. The temperature dependent development of the susceptibility between 25 and 295 K of Cu[μ_3-$O_3P(CH_2)_2COOH$]· $2H_2O$ (**1**) and Cu[(*RS*)-μ_3-$O_3PCH(C_2H_5)COOH$]·$3H_2O$ (**2**) (Figures 14 and 15) can be well fitted by an extended Curie-Weiss law as $\chi_{mol} = C\cdot(T-\Theta)^{-1}+\chi_0$.[45,46] For compound **1**, the Curie constant and the Weiss temperature were calculated as $C = 5.77\cdot10^{-6}$ m^3 K mol^{-1} and $\Theta = -0.19$ K. The temperature independent term is $\chi_0 = 0.0019$. The magnetic moment was calculated as $\mu_{eff} = 1.92(1)$ μ_B per Cu^{2+}. The deviation to the theoretical spin only value of 1.73 μ_B per Cu^{2+} is due to a weak spin-orbital interaction as often found in Cu^{2+} complexes.[47–49] As seen in the inset of Figure 14, below 25 K the magnetic moment decreases indicating a possible weak antiferromagnetic coupling between copper ions. The magnetic moment was calculated considering the Weiss temperature as $\mu_{eff}/\mu_B = 797.73[\chi_{mol}(T-\Theta)]^{0.5}$.[50] Since the copper cations are coordinated in a square pyramidal fashion, the magnetic orbital ($d_{x^2-y^2}$) pointing to the equatorial oxygen atoms O(3), O(4), O(5), and O(w2).[29] A direct exchange between adjacent Cu^{2+} ions can be excluded because of their large distance of 459.5(1) pm. The rather weak interaction can be obviously described by an antiferromagnetic Cu–O···O–Cu super-superexchange owing to the absence of Cu–O–Cu superexchange paths. The super-superexchange via the Cu–O(4)–P–O(3)–Cu paths, in which the oxygen atoms occupy the equatorial positions, is obviously responsible for the weak antiferromagnetic interaction (Figure 16). The equatorial planes of the copper square pyramids are parallel to each other. The strength of such spin exchange increases with decreasing O···O distances (smaller than the sum of the van der Waals radii), rising Cu–O···O angles, and a more parallel orientation of the magnetic orbitals.[51, 52] The O(4)···O(3) distance is 253.5(5) pm and the Cu–O(4)···O(3) and Cu–O(3)···O(4) angles account to 108.9(2)° and 133.4(2)°, respectively. The torsion angle of Cu–O(4)···O(3)–Cu is 69.9(3)°. Two further super-superexchange paths Cu–O(4)–P–O(5)–Cu and Cu–O(3)–P–O(5)–Cu with O···O distances of 255.3(4) and 248.6(4) pm can be neglected, because the equatorial planes of the copper centered polyhedra are tilted nearly orthogonal to each other [∠ 88.1(1)°].[52]

Compound **2** reveals a Curie constant of $C = 5.68\cdot10^{-6}$ m^3 K mol^{-1}, a Weiss temperature of $\Theta = -0.58$ K, and $\chi_0 = 0$. The calculated magnetic moment is $\mu_{eff} = 1.90(1)$ μ_B per Cu^{2+}. The inset in Figure 15 shows that the magnet moment decreases significantly below about 23 K. Analogous to **1**, the weak interaction between neighbouring copper ions at low temperatures is probably due a super-superexchange. A possible super-superexchange path is Cu–O(3)–P–O(5)–Cu (Figure 17) with a O(3)···O(5) distance of 250.3(4) pm, Cu–O(3)···O(5) and Cu–O(5)···O(3) angles of 137.7(2)° and 148.1(2)°, and a torsion angle of Cu–O(3)···O(5)–Cu of 158.7(3)°. The equatorial planes of the copper coordination polyhedra are almost parallel to each other [∠ 6.7(1)°]. Whereas, the equatorial planes of the two other possible exchange paths through Cu–O(4)–P–O(5)–Cu and Cu–O(3)–P–O(4)–Cu are tilted by 47.6(1)° and 48.1(1)° to each other and should only make a small contribution.

Such super-superexchange paths are also found in e.g. copper phosphates[53, 54], sodium copper methylenediphosphonate monohydrate[55], copper phosphonocarboxylates[15,26], and other copper phosphonates[56,57].

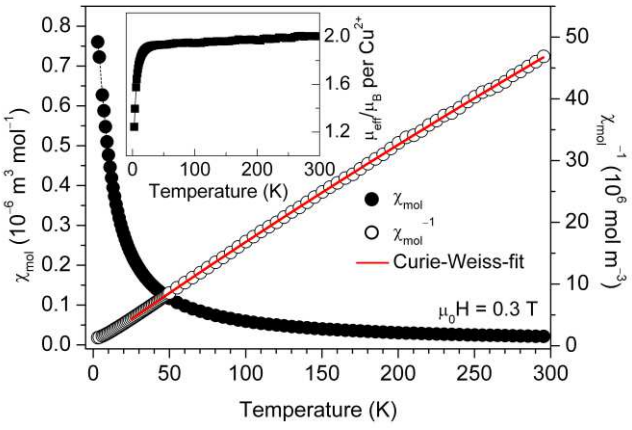

Figure 14. Susceptibility versus temperature of Cu[μ_3-$O_3P(CH_2)_2COOH$]·$2H_2O$ (**1**). The inset shows the temperature development of the magnetic moment in consideration of the Weiss temperature.

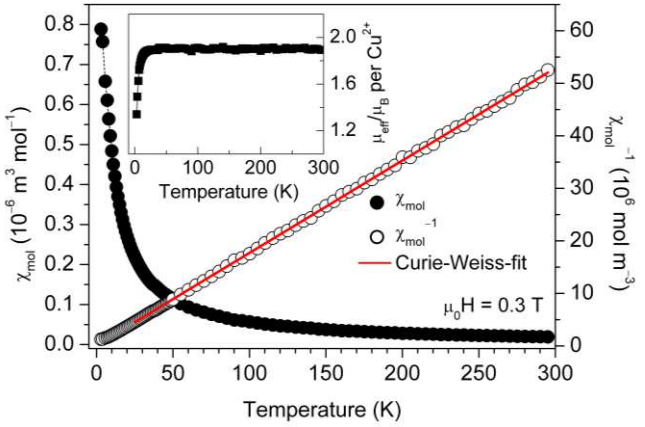

Figure 15. Susceptibility versus temperature of Cu[(*RS*)-μ_3-$O_3PCH(C_2H_5)COOH]\cdot 3H_2O$ (**2**). The inset shows the temperature development of the magnetic moment in consideration of the Weiss temperature.

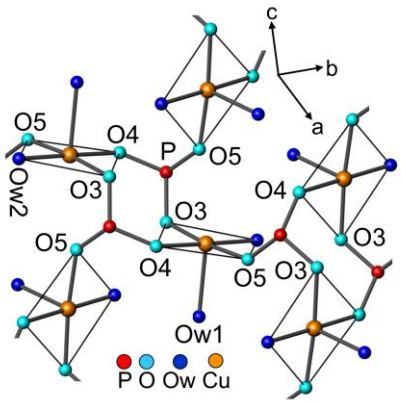

Figure 16. Connections between adjacent Cu^{2+} coordination polyhedra in Cu[μ_3-$O_3P(CH_2)_2COOH]\cdot 2H_2O$ (**1**). Carbon, hydrogen and oxygen atoms not bond to Cu^{2+} are omitted for clarity. Thin black lines illustrate the equatorial planes.

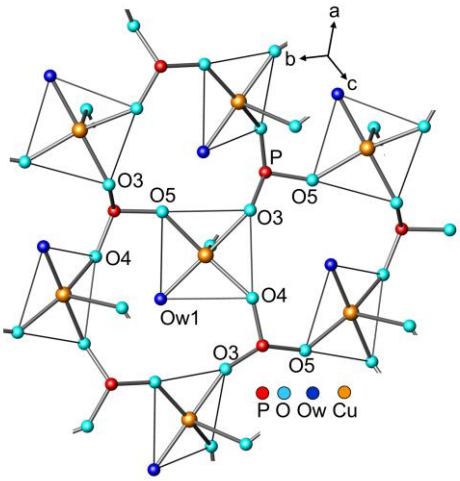

Figure 17. Connections between adjacent Cu^{2+} coordination polyhedra in Cu[(*RS*)-μ_3-$O_3PCH(C_2H_5)COOH]\cdot 3H_2O$ (**2**). Carbon, hydrogen and oxygen atoms not bond to Cu^{2+} are omitted for clarity. Thin black lines illustrate the equatorial planes.

The diffuse reflectance UV/Vis spectra for **1** and **2** are shown in Figure 18 and 19. Both compounds show a broad asymmetric band between 500 and 1400 nm representing d–d transitions. As seen in the inset in Figure 18, the d–d absorption band of **2** is slightly bathochromic shifted compared to **1**. The curve of compound **1** can be well fitted by three Gaussian curves with maxima at 743, 892, and 1016 nm. The Cu^{2+} centered square pyramid has C_{2v} point group symmetry, however the deviation from C_{4v} symmetry is negligible. Thus, the splitting of the ^2E energy level by reducing the symmetry from C_{4v} to C_{2v} can be neglected.[58,59] The ground state in C_{4V} (hole formalism) is $^2B_1$ and the energy level sequence is $^2B_1$ ($d_{x^2-y^2}$) < $^2A_1$ (d_{z^2}) < $^2B_2$ (d_{xy}) < ^2E (d_{xz},d_{yz}) leading to three transition bands.[60,61] The fitted absorption bands in **1** at 743 nm can be assigned as the $^2B_1 \rightarrow {}^2E$ transition, those at 892 nm as the $^2B_1 \rightarrow {}^2B_2$, and those at 1016 nm as the $^2B_1 \rightarrow {}^2A_1$ transition. The copper coordination polyhedron in **2** is considerably more distorted compared to the one in **1**. Due to the point group symmetry lower than C_{2v}, the spectrum of **2** can be well fitted by four Gaussian curves with maxima at 741, 838, 957, and 1151 nm.[28,29,58,62–64]

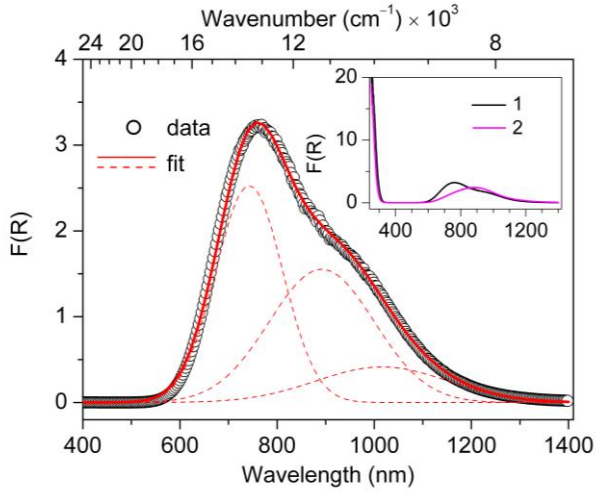

Figure 18. Diffuse reflectance UV/Vis spectrum of powdered Cu[(RS)-μ_3-$O_3P(CH_2)_2COOH]\cdot 2H_2O$ (**1**). Three Gaussian curves (red dashed lines) were used to fit the spectrum and their sum is presented by the thick red curve. The inset shows the spectra from 250 to 1400 nm of compound **1** and **2.** [F(R) = Kubelka-Munk-Function].

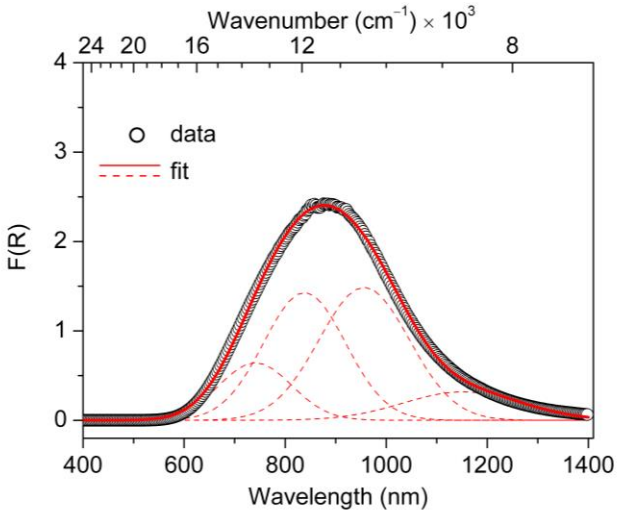

Figure 19. Diffuse reflectance UV/Vis spectrum of powdered Cu[(*RS*)-μ_3-$O_3PCH(C_2H_5)COOH]\cdot 3H_2O$ (**2**). Four Gaussian curves (red dashed lines) were used to fit the spectrum and their sum is presented by the thick red curve [F(R) = Kubelka-Munk-Function].

Conclusions

We reported on the crystal structure and properties of Cu[μ_3-$O_3P(CH_2)_2COOH]\cdot 2H_2O$ (**1**) and Cu[(*RS*)-μ_3-$O_3PCH(C_2H_5)COOH]\cdot 3H_2O$ (**2**). In both compounds the connection between the Cu^{2+} cations and the dianions of 3-phosphonopropionic acid and (*RS*)-2-phosphonobutyric acid, respectively, leads to infinite layers with features of cation exchangers. In **1**, the layers are interconnected by hydrogen bonds, whereas in **2** no hydrogen bonds exist between neighbouring layers. The UV/Vis spectra reveal d–d transition bands at 763, 878, 1061 nm for **1** and 741, 838, 957, 1151 nm for **2**, respectively. Magnetic measurements show a paramagnetic behaviour with an obviously weak antiferromagnetic interaction at low temperatures due to a super-superexchange coupling. The compounds are stable in air up to 95 °C (**1**) and 65 °C (**2**).

Experimental Section

Single crystals of Cu[μ_3-$O_3P(CH_2)_2COOH]\cdot 2H_2O$ (**1**) can be synthesized in aqueous solution. 0.002 mol 3-phosphonopropionic acid (2-carboxyethylphosphonic acid), 0.004 mol $Cu(SO_4)_2\cdot 5H_2O$ were dissolved in 10 ml deionized water. 1 M NaOH solution was added until a pH value of 2.5–3 was reached. To the clear solution, 90 mg urea was added and after several days at room temperature blue crystals appeared.[65] After filtering, the remaining filtrate was allowed to evaporate at room temperature yielding further blue crystals of **1**.

Crystals of Cu[(*RS*)-μ_3-$O_3P(C_2H_5$-CH)$COOH]\cdot 3H_2O$ (**2**) can be obtained from aqueous solution by dissolving 0.002 mol (*RS*)-2-phosphonobutyric acid (2-phosphonobutanoic acid) and 0.004 mol $Cu(SO_4)_2\cdot 5H_2O$ in 10 ml deionized water. The solution was adjusted to a pH value of about 3.5 with 1 M NaOH solution. After adding of 90 mg urea blue plate-like crystals of **2** occured after several days at room temperature.

IR (ATR): **1**: 3429 (w), 3000–2900 (s,broad), 2930 (w), 1686 (s), 1561 (m,broad), 1435 (w,sh), 1416 (m), 1343 (w), 1284 (w), 1246 (s), 1192 (s), 1146 (m), 1094 (s), 1051 (s), 1000 (s), 953 (w), 915 (w), 791 (m), 756 (m), 661 (w), 592 (w), 573 (m), 529 (m), 490 (m), 431 (w), 386 (m), 349 (m) cm^{-1}.

2: 3600–3000 (s,broad), 2964 (w), 2940 (w), 2881 (w), 1632 (s,broad), 1459 (m), 1384 (w), 1329 (m), 1299 (m), 1250 (m), 1186 (m), 1126 (w), 1061 (s), 1011 (s), 946 (w), 898 (m), 860 (m), 835 (m), 780 (m), 719 (m), 597 (w), 534 (m), 471 (m), 363 (m) cm^{-1}.

ATR Fourier transformed infrared (IR-ATR) measurements were carried out at room temperature with a resolution of 2 cm^{-1} using a Bruker Alpha FT-IR spectrometer equipped with diamond ATR unit. Thermoanalytic measurements with a heating rate of 10 K min^{-1} were performed in flowing air using a Netzsch STA 449F device. Temperature dependent magnetizations were measured at μ_0H = 0.3 T in the temperature range of 3 to 300 K using a Quantum Design PPMS 9. The magnetic data were corrected against the diamagnetic moment of the sample holder. The X-ray powder diffraction patterns were recorded at room temperature on a Bruker D8-Advance diffractometer, equipped with a one-dimensional silicon strip detector (LynxEye^{TM}) and operated with Cu-Kα radiation. The diffuse reflectance UV-Vis spectra were obtained using a Perkin Elmer UV/Vis spectrometer Lambda 19. $BaSO_4$ was used as a white standard. X-ray single crystal structure determination was performed on a Siemens P4 four-circle diffractometer (MoKα, graphite monochromator) in a theta range up to 24.00° and 22.50°, respectively. Face-indexed numerical absorption corrections have been applied. The phase problem was solved by direct methods. Full matrix least squares refinement employing $|F|^2$ made use of the SHELXTL program suite.[66] The C bound hydrogen atoms were positioned geometrically. The further hydrogen atom positions were located in Difference Fourier maps and refined with isotropic displacement parameters. Crystallographic data are compiled in Table 7. Further crystallographic data have been deposited with the Cambridge Crystallographic Data Centre, CCDC, 12 Union Road, Cambridge CB21EZ, UK. Copies of the data can be obtained free of

charge on quoting the depository number CCDC-1586605 (**1**) and 1586599 (**2**) (Fax: +44-1223-336-033; E-Mail: deposit@ccdc.cam.ac.uk, http://www.ccdc.cam.ac.uk).

Table 7. Crystallographic Data

Compound	**1**	**2**
Empirical formula	$C_3H_9PCuO_7$	$C_4H_{13}PCuO_8$
Crystal system	Orthorhombic	Orthorhombic
Space group	*Pbca* (no.61)	*Pbca* (no.61)
Lattice constants	a = 812.5(2) pm b = 919.00(9) pm *c* = 2102.3(2) pm	a = 1007.17(14) pm b = 961.2(3) pm *c* = 2180.9(4) pm
Cell volume	1.5697(4) nm^3	2.1112(8) nm^3
Formulas in unit cell	8	8
Formula weight	251.61 g mol^{-1}	283.65 g mol^{-1}
Density (calc.)	2.129 g cm^{-3}	1.785 g cm^{-3}
Wavelength	71.073 pm	
Absorption coefficient	2.985 mm^{-1}	2.237 mm^{-1}
Numerical absorption correction	min./max. transmittance 0.69573/0.97062	min./max. transmittance 0.77044/0.95621
Temperature	293(2) K	
Crystal size (mm)	0.14 x 0.14 x 0.01	0.22 x 0.12 x 0.02
F (000)	1016	1160
Θ-range	3.17° – 24.00°	2.75° – 22.50°
Limiting indices	h: -1/+9; k: -1/+10; l: -1/+24	h: 0/+10; k: 0/+10; l: -23/+23
Reflections collected	1700	2922
Independent reflections	1231 (R_{int} = 0.0564)	1378 (R_{int} = 0.0440)
Structure solution	Direct methods	
Structure refinement	Full-matrix least-squares on $\|F\|^2$	
Refined parameters	128	153
Final max. shift/esd Final mean shift/esd	0.001 0.000	-0.001 0.000
Goodness-of-fit on $\|F\|^2$	0.600	1.098
Residuals (all data)	R_1 = 0.0740 , wR_2 = 0.0569	R_1 = 0.0565 , wR_2 = 0.0726
Max. features in last Difference Fourier synthesis	374 and -356 e·nm^{-3}	478 and -576 e·nm^{-3}

Supporting Information (see footnote on the first page of this article): Crystal structure of compound **2** viewed on (100) (Figure S1). XRD powder patterns of compound **1** and **2** and of decomposition products after heating at 175 °C and 200 °C, respectively (Figures S2 and S3).

Acknowledgements

One of the authors (R.K.) is thankful to the German Research Foundation (DFG) within the Collaborative Research Centre (SFB 762) *Functionality of Oxide Interfaces* for financial support.

Keywords: 3-Phosphonopropionic acid • 2-Phosphonobutyric acid • Coordination polymer • Crystal structure • UV-Vis spectroscopy

References

[1] L.C. Brousseau III and T.E. Mallouk, *Anal. Chem.* **1997**, *69*, 679–687.
[2] H. Byrd, A. Clearfield, D. Poojary, K.P. Reis, M.E. Thompson, *Chem. Mater.* **1996**, *8*, 2239–2246.
[3] M.E. Thompson, *Chem. Mater.* **1994**, *16*, 1168–1175.
[4] C.-Y. Yang and A. Clearfield, *React. Polym.* **1987**, *5*, 13–21.
[5] M. Deng, Y. Ling, B. Xia, Z. Chen, Y. Zhou, X. Liu, B. Yue, H. He, *Chem. Eur. J.* **2011**, *17*, 10323–10328.
[6] T.-B. Liao, Y. Ling, Z.-X. Chen, Y.-M. Zhou, L.-H. Weng, *Chem. Comm.* **2010**, *46*, 1100–1102
[7] A. N. Alsobrook, B. G. Hauser, J. T. Hupp, E. V. Alekseev, W. Depmeier, T. E. Albrecht-Schmitt., *Chem. Comm.* **2010**, *46*, 9167–9169.
[8] W. Dan, X. Liu, M. Deng, Y. Ling, Z. Chen, Y. Zhou, *Dalton Trans.* **2015**, *44*, 3794–3800.
[9] A. I. Bortum, L. Bortum, A. Clearfield, E. Jaimez, M. A. Villa-García, J. R. García, J. Rodríguez, *J. Mater. Res.* **1997**, *12*, 1122–1130.
[10] N. Muchanyereyi and R. M. Tindwa, *Phys. Rev. Res. Int.* **2012**, *2*, 22–35.
[11] R. Silbernagel, C. H. Martin, A. Clearfield, *Inorg. Chem.* **2016**, *55*, 1651–1656.
[12] T. Zhou, D. Wang, S. Chun-Kiat Goh, J. Hong, J. Han, J. Mao, R. Xu, *Energy Environ. Sci.* **2015**, *89*, 526–534.
[13] M. S. M Abdelbaky, Z. Amghouz, D. M. Blanco, S. García-Granda, J. R. García, *J. Solid State Chem.* **2017**, *248*, 61–67.
[14] X.-M. Zhang, *Eur J. Inorg. Chem.* **2004**, 544–548.
[15] R. Köferstein, M. Arnold, C. Robl, *Z. Anorg. Allg. Chem.* **2017**, *643*, 276–285.
[16] K. E. Knope and C. L. Cahill, *Inorg. Chem.* **2008**, *47*, 7660–7672.
[17] B. Bujoli, A. Courilleau, P. Palvaeau, J. Rouxel, *Eur. J. Solid State Inorg. Chem.* **1992**, *29*, 171–182.
[18] S. Drumel, P. Janvier, P. Barboux, M. Bujoli-Doeuff, B. Bujoli, *Inorg. Chem.* **1995**, *34*, 148–156.
[19] A. Distler and S. C. Sevov, *Chem. Comm.* **1998**, 959–960.
[20] P. A. Britel, J. C. Boivin, D. Thomas, M. Wozniak, *Acta Cryst.* **1985**, *C45*, 1609–1612.
[21] S. Ayyappan, G. Diaz de Delgado, A. K. Cheethman, G. Férey, C. N. R. Rao, *J. Chem. Soc., Dalton Trans.* **1999**, 2905–2907.
[22] N. Stock, G. D. Stucky, A. K. Cheetham, *Chem. Comm.* **2000**, 2277–2278.
[23] F. Fredoueil, M. Evain, D. Massiot, M. Bujoli-Doeuff, P. Janvier, A. Clearfield, B. Bujoli, *J. Chem. Soc., Dalton Trans.* **2002**, 1508–1512.
[24] M. Mar Gómez-Alcantara, M. A. G. Aranda, P. Olivera-Pastor, P. Beran, J. L. Garćia-Muñoz, A. Cabeza, *Dalton Trans.* **2006**, 577–585.

[25] E. Fernández-Zapico, J. M. Montejo-Bernardo, R. D´Vries, J. R. García, S. García-Granda, J. R. Fernández, O. de Pedro, J. A. Blanco, *J. Solid State Chem.* **2011**, *184*, 3289–3298.
[26] F. A. Mautner, M. Salah El Fallah, S. Speed, R. Vicente, *Polyhedron* **2014**, *81*, 1–5.
[27] Z. Chen, L. Weng, D. Zhao, *Inorg. Chem. Comm.* **2007**, *10*, 447–450.
[28] B.J. Hathaway, in *Comprehensive Coordination Chemistry*, (Ed. G. Wilkinson) Pergamon Press, Oxford **1985**, vol. 5, p. 533–774.
[29] B.J. Hathaway and D.E. Billing, *Coord. Chem. Rev.* **1970**, *5*, 143–207.
[30] A. Pasquarello, I. Petri, P.S. Salmon, O. Parisel, R. Car, E. Tóth, D. H. Powell, H. E. Fischer, L. Helm, A. E. Merbach, *Science* **2001**, *291*, 856–859.
[31] N. E. Brese and M. O'Keeffe, *Acta Cryst.* **1991**, *B47*, 192–197.
[32] F.H. Allen, O. Kennard, D.G. Watson, L. Brammer, A.G. Orpen, R. Taylor, *J. Chem. Soc. Perkin Trans. II* **1987**, S1–S19.
[33] M. Riou-Caellec, M. Sanselme, N. Guillou, G. Férey, *Inorg. Chem.* **2001,** *40*, 723–725.
[34] X.-M. Zhang, R.-Q. Fang, H.-S. Wu, S. W. Ng, *Acta Cryst.* **2003**, *E59*, m1149–m1150.
[35] A. Weiss, *Chem. Ber.* **1958**, *91*, 487–502.
[36] M. Riou-Cavellec, M. Sanselme, J.-M. Grenèche, G. Ferey, *Solid State Sci.* **2000**, *2*, 717–724.
[37] F. Fredouli, D. Massiot, D. Poojary, M. Bujoli-Doeuff, A. Clearfield, B. Bujoli, *Chem. Comm.* **1998**, 175–176.
[38] R. M. P. Colodrero, A. Cabeza, P. Olivera-Pastor, M. Papadaki, J. Rius, D. Choquesillo-Lazarte, J. M. García-Riuz, K. D. Demadis, M. A. G. Aranda, *Cryst. Growth Des.* **2011**, *11*, 1713–1722.
[39] W. Klyne and V. Prelog, *Experientia* **1960**, *16*, 521–568.
[40] K. Moedritzer and R. R. Irani, *J. Inorg. Nucl. Chem.* **1961**, *22*, 297–304.
[41] A. W. Herlinger, J. R. Ferraro, J. A. Garcia, R. Chiarizia, *Polyhedron* **1998**, *17*, 1471–1475.
[42] K.-R. Ma, C.-Li. Wei, Y. Zhang, Y.-H. Kan, M.-H. Cong, X.-J. Yang, *J. Spectros.* **2013**, 378379.
[43] R. Luschtinetz, G. Seifert, E. Jaehne, H.-J. P. Adler, *Macromol. Symp.* **2007**, *254*, 248–253.
[44] L. W. Daasch and D. C. Smith, *Anal. Chem.* **1951**, *23*, 853–868.
[45] A. Arrott, *J. Appl. Phys.* **1958**, *29*, 508–512.
[46] R. Köferstein, T. Buttlar, S. G. Ebbinghaus, *J. Solid State Chem.* **2014**, *217*, 50–56.
[47] G. S. Manku, *Theoretical Principles in Inorganic Chemistry*, Tata McGraw-Hill Publishing Company, New Dehli, **2006**. p. 532 et seq.
[48] B. N. Figgis and J. Lewis, *Prog. Inorg. Chem.* **1964**, *6*, 237–239.
[49] R. Köferstein and C. Robl, *Z. Anorg. Allg. Chem.* **2015**, *641*, 1886–1891.
[50] D. Mastropaolo, D. A. Powers, J. A. Potenza, H. J. Schugar, *Inorg. Chem.* **1976**, *15*, 1444–1449.
[51] H.-J. Koo and M.-H. Whanbo, *Inorg. Chem.* **2001**, *40*, 2161–2169.
[52] Y. Chen, T. Liu, C. He, C. Duan, *J. Mater. Chem.* **2012**, *22*, 19872–19881.
[53] H.-J. Koo, D. Dai, M.-H. Whangbo, *Inorg. Chem.* **2005**, *44*, 4359**–**4365.
[54] A. A. Belik, M. Azuma, A. Matsuo, M.-H. Whangbo, H.-J. Koo, J. Kikuchi, T. Kaji, S. Okubo, H. Ohta, K. Kindo, M. Takano, *Inorg. Chem.* **2005**, *44*, 6632–6640.
[55] K. Bathelet, M. Nogues, D. Riou, G. Férey, *Chem. Mater.* **2002**, *14*, 4910–4918.
[56] H. Zhu, J. Huang, S.-S. Bao, M. Ren, L.-M. Zheng, *CrystEngComm..* **2013**, *15*, 10316–10322.
[57] J. Huang, P.-Y. Liu, H. Zhu, S.-S. Bao, L.-M. Zheng, J. Ma, *ChemPlusChem* **2012**, *77*, 1087–1095.
[58] D. Reinen and M. Atanasov, *Chem. Phys.* **1989**, *136*, 27–46.
[59] F. A. Walker, *Coord. Chem. Rev.* **1999**, *185–186*, 471–534.
[60] E. A. Boudreaux, *Trans. Faraday Soc.* **1963**, *59*, 1055–1058.
[61] B. J. Hataway and A. A. G. Tomlinson, *Coord. Chem. Rev.* **1970**, *5*, 1–43.
[62] T. Murakami, T. Takei, Y. Ishikawa, *Polyhedron* **1997**, *16*, 89–93.
[63] I. I. Volchenskova, *Theor. Exp. Chem.* **1975**, *9*, 495–501.
[64] P. Sivaprasad, K. Ramesh, Y. P. Reddy, *Phys. Status Solidi A* **1990**, *118*, K103–K106.
[65] M. Arnold, Dissertation, Universität Jena, Germany, **1998**.
[66] G. M. Sheldrick, *Acta Cryst.* **2008**, *A64*, 112–122.

Received: ((will be filled in by the editorial staff))
Published online: ((will be filled in by the editorial staff))

Supporting Information:

Crystal Structure and Characterization of Two Layered Copper(II) Coordination Polymers with Anions of 3-Phosphonopropionic Acid and (*RS*)-2-Phosphonobutyric Acid

Roberto Köferstein[b], Michael Arnold[b] and Christian Robl*[a]

[a] *Institute of Inorganic and Analytical Chemistry, Friedrich-Schiller-University Jena, Humboldtstrasse 8, 07743 Jena, Germany.*
[b] *Institute of Chemistry, Inorganic Chemistry, Martin Luther University Halle-Wittenberg, Kurt-Mothes-Strasse 2, 06120 Halle, Germany.*

* *Corresponding author. E-mail address: crr@uni-jena.de*

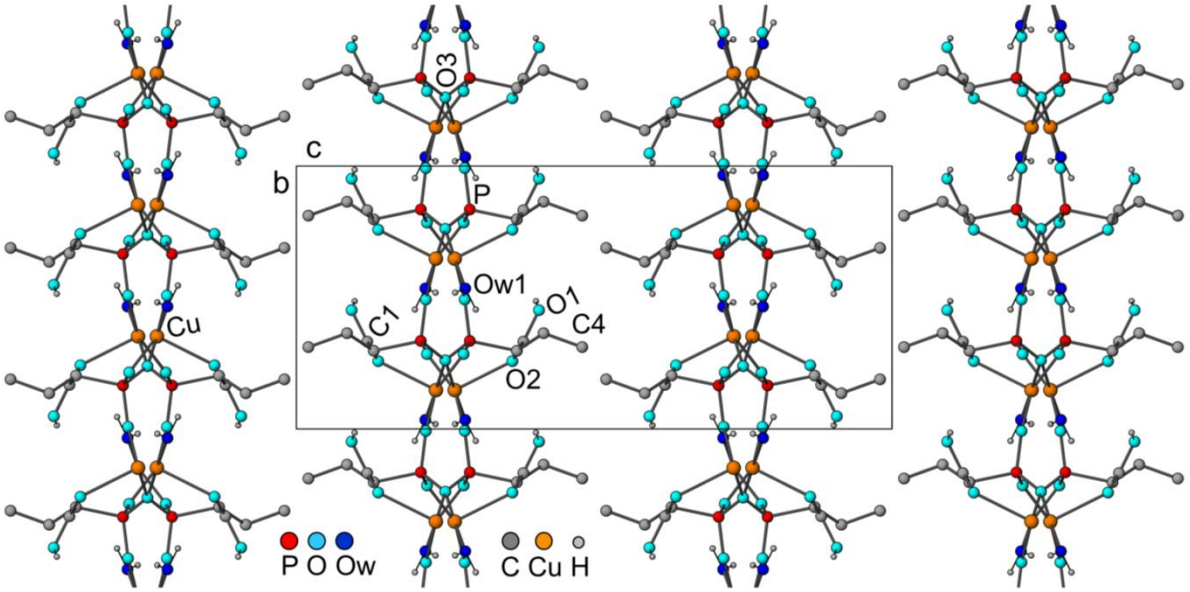

Figure S1. Crystal structure of Cu[(*RS*)-μ_3-$O_3PCH(C_2H_5)COOH]\cdot 3H_2O$ (**2**) viewed from [100]. The uncoordinated water molecules O(w2) and O(w3) and all hydrogen atoms bound to carbon atoms are omitted for clarity.

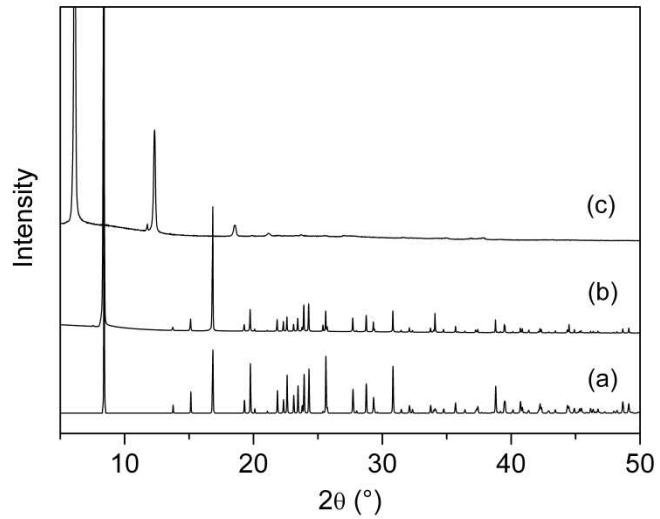

Figure S2. X-ray powder diffraction patterns of $Cu[\mu_3\text{-}O_3P(CH_2)_2COOH]\cdot 2H_2O$ (**1**). (a) calculated pattern, (b) experimental pattern, c) pattern after heating at 175 °C.

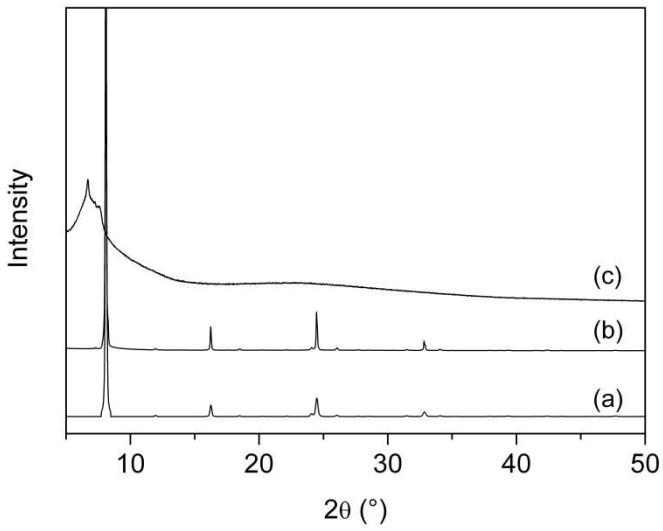

Figure S3. X-ray powder diffraction patterns of $Cu[(\textit{RS})\text{-}\mu_3\text{-}O_3PCH(C_2H_5)COOH]\cdot 3H_2O$ (**2**). (a) calculated pattern, (b) experimental pattern, c) pattern after heating at 200 °C. The pattern of graph (a) was calculated using the March-Dollase model with a (001) preferred orientation.